IEEE Photonics Journal
An IEEE Photonics Society Publication

Label-Free Biosensing With a Slot-Waveguide-Based Ring Resonator in Silicon on Insulator

Volume 1, Number 3, September 2009

Tom Claes
Jordi Gironès Molera
Katrien De Vos
Etienne Schacht
Roel Baets
Peter Bienstman

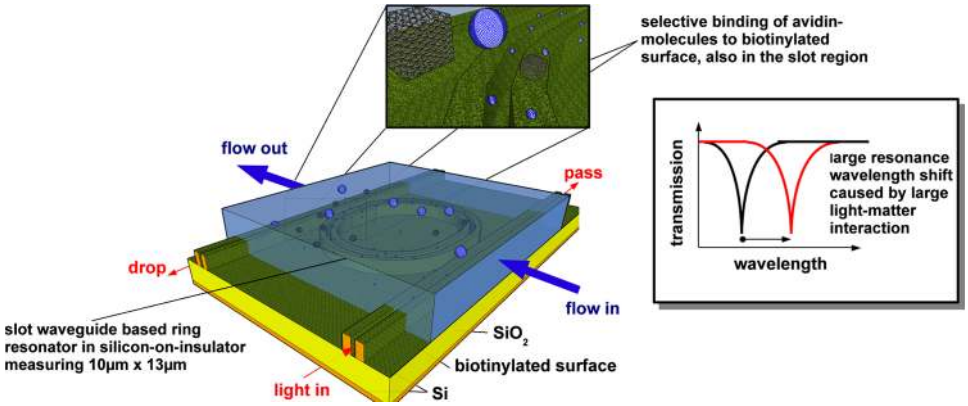

DOI: 10.1109/JPHOT.2009.2031596
1943-0655/$26.00 ©2009 IEEE

Label-Free Biosensing With a Slot-Waveguide-Based Ring Resonator in Silicon on Insulator

Tom Claes,[1] Jordi Gironès Molera,[2] Katrien De Vos,[1] Etienne Schacht,[2] Roel Baets,[1] and Peter Bienstman[1]

[1]Photonics Research Group, Department of Information Technology, Ghent University—IMEC, 9000 Gent, Belgium
[2]Polymer Chemistry and Biomaterials Research Group, Department of Organic Chemistry, Ghent University, 9000 Gent, Belgium

DOI: 10.1109/JPHOT.2009.2031596

Manuscript received June 15, 2009; revised August 11, 2009. First published Online August 28, 2009. Current version published September 18, 2009. This work was supported in part by Ghent University through the GOA project B/05958/01 and was performed in the context of the Belgian IAP project Photonics@BE and the European FP7 project InTopSens. T. Claes and K. De Vos were supported by the Flemish Institute for the Promotion of Innovation through Science and Technology (IWT) with a specialization grant. Corresponding author: T. Claes (e-mail: tom.claes@intec.ugent.be).

Abstract: We present a slot-waveguide-based ring resonator in silicon on insulator (SOI) with a footprint of only 13 μm $\times$ 10 μm, fabricated with optical lithography. Experiments show that it has 298 nm/RIU sensitivity and a detection limit of $4.2 \cdot 10^{-5}$ RIU for changes in the refractive index of the top cladding. We prove for the first time that surface chemistry for selective label-free sensing of proteins can be applied inside a 100 nm-wide slot region and demonstrate that the application of a slot waveguide instead of a normal waveguide increases the sensitivity of an SOI ring resonator with a factor 3.5 for the detection of proteins.

Index Terms: Biosensor, ring resonator, silicon on insulator, slot waveguide.

1. Introduction

Integrated label-free optical biosensors can contribute to major advances in medical diagnostics, food quality control, drug development, and environmental monitoring and offer the prospect of being incorporated in laboratories on a chip [1]. These chips often have to provide multiparameter analysis, for which they need to harbor many compact and sensitive sensors and, therefore, are preferably made in a high-index-contrast material system. Additionally, the sensor chips usually need to be disposable, meaning that the chip will only be used once in order to avoid complex cleaning of the sensor surface after use [2]. Therefore, fabrication of the photonic chip needs to be cheap, which can be achieved by making the chips in high volume with mass fabrication techniques.

In [3], we described a silicon-on-insulator (SOI) ring resonator, which has 70 nm/RIU sensitivity for bulk changes of the refractive index and showed a 625 pm saturation shift of the resonance wavelength for label-free sensing of proteins with the well-known strong affinity couple biotin/avidin. In this paper, we present a more sensitive sensor in which the light-matter interaction is improved by the use of slot waveguides. This are waveguides with a narrow low-refractive-index region in between two ribs with high refractive index, which are known to enhance the transverse-electric (TE) polarized field in the low-index slot region [4].

The authors in [5] presented a slot-waveguide-based ring resonator for biosensing in the low-index-contrast material system Si_3N_4 on SiO_2 with 140 μm $\times$ 140 μm footprint and a 200 nm-wide slot region. It showed to have 212 nm/RIU sensitivity and was characterized for label-free sensing with BSA/anti-BSA in [6].

The novel aspects we present in this paper are twofold. First, we show a device with comparable performance to the sensor presented in [5] and [6] but with a 150-time smaller footprint that has been fabricated in the high-index-contrast material system SOI. We think this is an important step toward integration of this kind of sensor in a sensor matrix. Also, it is fabricated using mass fabrication compatible optical lithography, which opens the way toward cheap, disposable chips. Second, we prove for the very first time that it is possible to apply surface chemistry inside a slot region that is only 100 nm wide. This is of great importance for the application of nanophotonics for biosensing.

2. Toward More Sensitive Resonant Waveguide-Based Label-Free Biosensors

A waveguide-based resonator can be used as a biosensor by applying a proper surface chemistry to the waveguide surface. This will result in a thin layer on top of the waveguide that contains receptor molecules that are specific to the analyte, the molecule that one wants to detect. When the resonator is brought into contact with a fluid containing this analyte, the analyte will bind to the receptor molecules at the surface of the waveguide, causing a thickness change of the layer on top of the waveguide. The effective index of the resonator waveguide mode will change proportionally to the number of binding events, resulting in a corresponding change of the resonance wavelength

$$\Delta\lambda = \frac{\Delta n_{eff} \cdot \lambda_{res}}{n_g} \tag{1}$$

where Δn_{eff} is the change of the effective index caused by the analyte binding, λ_{res} is the initial resonance wavelength, and n_g is the group index. By using the group index in the nominator instead of the effective index, first-order dispersion is taken into account.

This model is valid when the number of binding events is large enough to assume uniform binding of the analyte to the sensor surface. When approaching single-molecule detection, the effective index change Δn_{eff} will typically depend on the exact binding locations of the analyte molecules. As the detection limit of the sensor described in this article is far from the single-molecule detection limit, we can work with this model.

There are two important routes to improve the detection limit of the sensor: one approach is to maximize the quality factor of the resonator, which will decrease the impact of noise on the determination of the resonance wavelength [7]. Another approach is to maximize the average resonance wavelength shift per binding event by increasing the interaction of light and biomolecules that get attached to the waveguide surface. When using a normal photonic waveguide with a rectangular cross section, only the evanescent tail of the waveguide mode will interact with the biomolecules. By etching a narrow slot in the middle of the waveguide, however, a vast fraction of the quasi-TE mode will be concentrated in that slot [4], causing it to have more interaction with analyte molecules binding to the waveguide surface in the slot region and improving the sensitivity of the sensor.

3. Optimization of Silicon Slot Waveguides for Label-Free Biosensing

Using the film mode matching tool *Fimmwave* [8], we optimized the slot width and rib width of a silicon slot waveguide for label-free biosensing of proteins. As will be explained in Section 4.2, we experimentally characterized our sensor by sensing the interaction of avidin with biotin attached to the surface of our resonator. For the optimization in this section, we used a simple model of this experiment:

Before the slot waveguide is brought into contact with avidin, we model it based on the physical parameters of our wafers as a 220 nm-high silicon waveguide completely covered with a 4.5 nm-thick

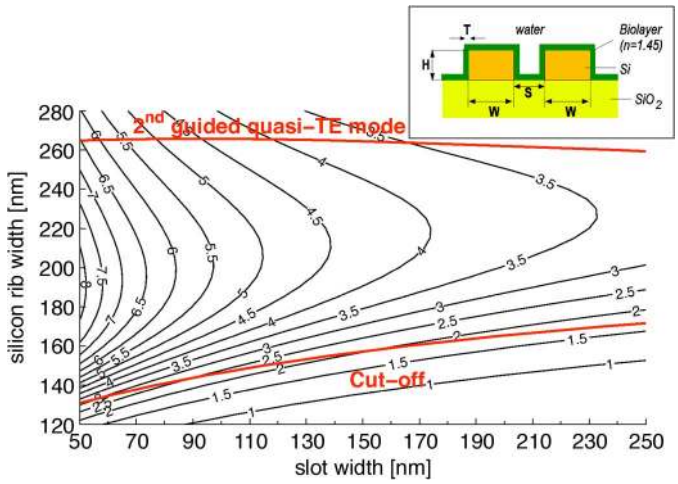

Fig. 1. Theoretical shift (nm) of a resonant biosensor based on a silicon slot waveguide as a function of the slot width S and rib width W of the waveguide when the sensor is saturated with proteins. The single-mode regime for the quasi-TE polarization is indicated.

layer with refractive index 1.45 (see the inset in Fig. 1), which represents 2 nm native oxide and 2.5 nm functional layer with receptor molecules [9], [10]. Complete saturation of the slot waveguide with avidin, when all the binding sites at the waveguide surface are occupied, can be modeled by an additional 5 nm layer with refractive index 1.45 [10].

Note the importance of simulating changes at the surface of the waveguide for the optimization, rather than simulating changes of the bulk refractive index of the top cladding of the waveguide. The latter would result in a waveguide with maximal power fraction in the top cladding, while for label-free sensing, the interaction of light with surface changes is more important.

As a function of slot width and rib width, the effective index of the waveguide was simulated once for 4.5 nm biolayer thickness (model for initial surface chemistry) and once for 9.5 nm biolayer thickness (model for saturated surface). By using (1), the difference in effective index, $\Delta n_{eff} = n_{eff,9.5\ \mathrm{nm}} - n_{eff,4.5\ \mathrm{nm}}$, was used to calculated the expected resonance wavelength shift of a resonator based on this slot waveguide.

The contour plot in Fig. 1 shows the calculated resonance wavelength shift as a function of slot width and rib width. In this range of the parameters, the sensitivity increases with decreasing slot width. A slot width down to 100 nm is feasible with our technology. When in that case the silicon rib width is chosen to be 210 nm, our simulation shows that a 5.4 nm resonance wavelength shift at saturation of the biosensor is achievable. A similar simulation on a normal 500 nm-wide silicon wire, as used in [3], shows that the optimal slot waveguide presented here can increase the sensitivity of a wire-based sensor by a factor of 8.

4. Experimental Characterization of the Sensor

We present a ring resonator comprised of SOI slot waveguides with 104 nm slot width and, unfortunately, a suboptimal 268 nm rib width. The device is fabricated with 193 nm optical lithography [11], and is displayed in Fig. 2. Its waveguides are 220 nm high and are separated from the silicon substrate by 2 μm buffer oxide. The ring has a 5 μm bending radius and two access waveguides. To enhance the coupling efficiency in the directional couplers, the access waveguides are identical to the ring resonator slot waveguide. The mode conversion between the fundamental quasi-TE mode of a normal waveguide, and that of the access slot waveguide is done by an 8 μm-long adiabatic taper [12].

In our experiments, the input and output signals were carried by single-mode fibers that were quasi-vertically coupled to the photonic chip using grating couplers [11]. The polarization was tuned for maximum coupling to the fundamental quasi-TE mode of the silicon waveguides by using

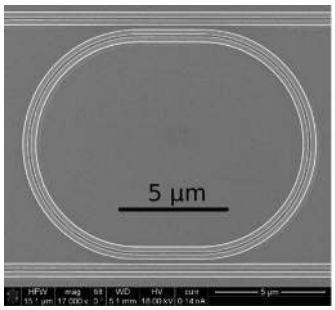

Fig. 2. Top-view scanning electron microscope image of the slot-waveguide-based ring resonator.

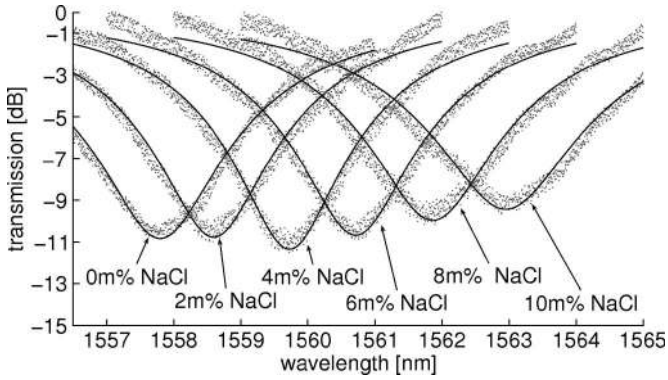

Fig. 3. Resonance dip in the pass spectrum of the slot-waveguide-based ring resonator for different salt concentrations. The measured spectrum is shown in gray, while the Lorentzian fits are shown in black.

polarization controllers. The temperature of the chip was fixed at 20 °C with a Peltier cooler. When characterizing the sensor for bulk refractive index sensing (see Section 4.1), the pass spectrum of the ring resonator was analyzed with 5 pm resolution by using a tunable laser and power detector. In the protein interaction experiment (see Section 4.2), light was generated with a super luminescent LED with its central wavelength at 1530 nm and the pass spectrum of the ring resonator was measured every 10 s with an optical spectrum analyzer with 100 pm resolution. The alignment of the input and output optical fibers was fixed in that experiment by gluing them to the grating couplers with ultraviolet-curable glue.

4.1. Sensing Refractive Index Changes in the Top Cladding

We measured the sensitivity for refractive index changes in the complete top cladding of this slot-waveguide-based ring resonator by flowing aqueous NaCl-solutions with different concentrations over the sensor. We used a flow cell with a 7 mm^3 closed channel to control the concentration by avoiding evaporation and to allow easy switching between different liquids. The sensor surface was not chemically modified for this experiment. Fig. 3 shows the shift of a resonance dip in the pass spectrum of the ring resonator when different salt concentrations are flown over. Lorentzian fitting was used to determine the resonance wavelength.

Fig. 4 shows the linear shift of the resonance wavelength as a function of the top cladding index, where the refractive index of the salt solutions at a wavelength of 1550 nm [13] was used. The sensitivity of the slot-waveguide-based ring resonator with 104 nm slot width and 268 nm silicon rib width is 298 nm/RIU as compared to 70 nm/RIU for a normal-waveguide-based ring resonator [3].

As it is often a matter of debate whether water enters a 100 nm-sized slot region or not, we simulated the effective index change of our slot waveguide for changing the top cladding index using the film mode matching tool *Fimmwave* [8], once assuming the slot region to be completely

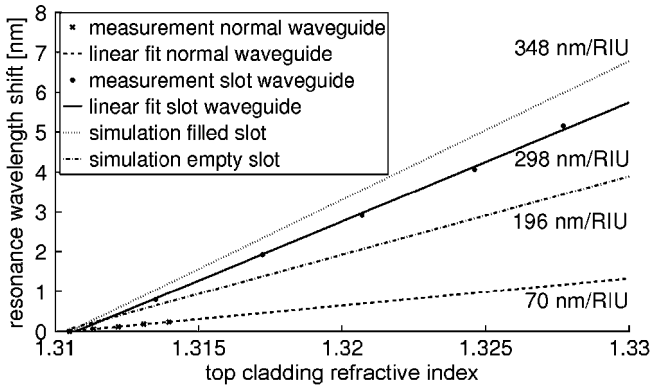

Fig. 4. Comparison between the experimental resonance wavelength shift of a normal-waveguide-based ring resonator [3] and the theoretical and experimental resonance wavelength shift of our slot-waveguide-based ring resonator as a function of the top refractive index.

filled with liquid and once assuming it not to be filled at all. By using formula (1), this, respectively, resulted in theoretical sensitivities of 348 nm/RIU and 196 nm/RIU. As our experimentally determined sensitivity lies in between these values, this indicates that the slot is partially filled.

Another important characteristic of a sensor is its detection limit, the smallest change in the refractive index that can still be resolved, which is equal to the resonance wavelength resolution divided by the sensitivity [7]. The resonance wavelength resolution is not only influenced by the resolution of the measurement equipment but also by the quality factor and extinction of the resonator and by the amount of noise on the measured spectrum, which causes uncertainty to exist on the resonance wavelength determined by fitting a Lorentzian curve to the measured resonance dip. In [7] it is shown that the noise is mainly dominated by Gaussian intensity noise. In this case the actual, but unknown, resonance wavelength can, based on a single measurement, in good approximation be assumed to be normally distributed with its mean equal to the fitted wavelength and its standard deviation equal to half of the 68.28% confidence interval of the fitted wavelength, which can be calculated by standard curve-fitting software and is a property of a normal distribution.

If the resonance wavelength of the sensor is determined two consecutive times and the second fitted resonance wavelength has shifted by $\Delta\lambda$ compared to the one in the first measurement, the probability that this shift is caused by a change of the refractive index is equal to

$$Prob[detection] = 1 - \frac{\int N(\lambda,\sigma)N(\lambda-\Delta\lambda,\sigma)d\lambda}{\int N^2(\lambda,\sigma)d\lambda} \tag{2}$$

with $N(\lambda,\sigma)$ the normal distribution of the resonance wavelength with mean λ and standard deviation σ. The second term in this equation represents the overlap between the distribution of both measurements.

If we define the resonance wavelength resolution as the shift $\Delta\lambda$ for which we are 95% sure of a detection, it follows from (2) that this resonance wavelength resolution is 3.5 times the standard deviation of the resonance wavelength distribution or 1.75 times the 68.28% confidence interval of the fitted wavelength.

For our sensor, this calculation results in a resonance wavelength resolution of 12.5 pm. Consequently, the detection limit is $(12.5\ \text{pm}/298\ \text{nm/RIU}) = 4.2 \cdot 10^{-5}$ RIU.

4.2. Label-Free Sensing of Proteins

In this experiment, the chip surface was silanized with 3-glycidyloxypropyltrimethoxysilane (GOPTS) following the procedure published before [14], and biotin receptor molecules were immobilized by immersing the GOPTS treated chips overnight in a 0.2 mg/ml solution of 5-(biotinamido)-pentylamine in phosphate buffered saline (pH 9.0).

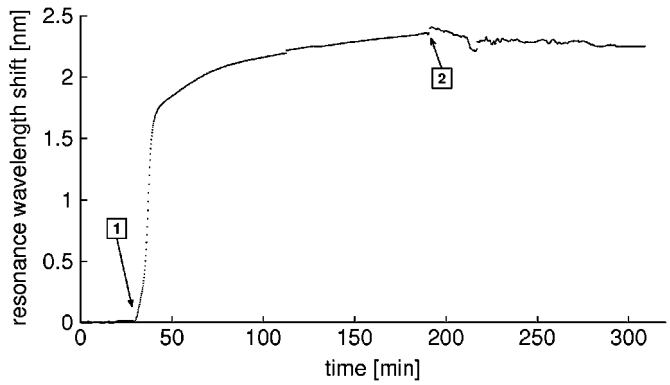

Fig. 5. Resonance wavelength shift of our slot-waveguide-based ring resonator caused by avidin molecules binding to biotin receptors immobilized at the surface. 1. Switch from HBS buffer liquid to 100 μg/ml avidin dissolved in HBS. 2. Switch to HBS again to rinse the sensor.

Using a 7 mm^3 flow cell and a syringe pump, HEPES-buffered saline (HBS) was flowed over the sensor at 10 μl/min to measure the reference resonance wavelength to be 1548.5 nm. Then a solution of 100 μg/ml avidin in HBS was flowed over the sensor, while the pass spectrum of the ring resonator was measured every 10 s. Fig. 5 shows that the resonance wavelength, determined by Lorentzian fitting, shifts toward larger wavelengths as avidin molecules attach to the sensor surface. After 1.7 ml of the avidin solution was flown over the ring resonator, HBS without avidin was flown over again to rinse the surface. As can be seen in Fig. 5, the resonance wavelength is permanently shifted by 2.2 nm, proving that the shift is caused by attached avidin molecules. The erratic behavior of the resonance wavelength short after switching is caused by an air bubble introduced during switching.

As shown in [3], for similar flow volumes as we used here, the shift of a normal-waveguide-based resonator in SOI becomes independent of the avidin concentration for concentrations larger than 10 μg/ml, as the sensor will then be completely saturated. As we have worked here with a similar surface chemistry, and with 100 μg/ml avidin concentration, we can conclude that we are far in the saturation regime of our sensor. The saturation shift of a normal-waveguide-based ring resonator in SOI is 625 pm [3], while we measured 2.2 nm for a slot-waveguide-based ring resonator, proving that our new sensor is 3.5 times more sensitive than the previous one.

Our simulations of a waveguide with the same dimensions as the fabricated one, with the method described in Section 3, predict a 4.45 nm saturation shift of the resonance wavelength when the avidin molecules bind uniformly to the sensor surface, including inside the slot region. When assuming that the avidin molecules only bind outside the slot region, and that the slot region is not filled with liquid, a similar simulation predicts a 1.3 nm saturation shift. As our experimentally determined saturation shift of 2.2 nm lies in between those two theoretical values, we can conclude that there are indeed avidin molecules interacting with a biochemical layer inside the slot region. It also indicates that the surface coverage inside the slot region can still be further improved, which might be achieved by optimizing the chemical reaction parameters of the surface modification procedure specifically for the geometry and roughness of the slot waveguide and by using more advanced on-chip fluidics.

5. Future Improvements

Compared with a normal-waveguide-based ring resonator, this slot-waveguide-based ring resonator has an increased sensitivity, but this has not yet translated into a corresponding increase of the detection limit. This is mainly caused by the small quality factor of this resonator.

To calculate the influence of the quality factor on the detection limit, we simulated the resonance dip of our sensor to be a Lorentzian curve with the same extinction as the measured resonance dips depicted in Fig. 3 and added Gaussian noise to it with the same noise energy as the measured

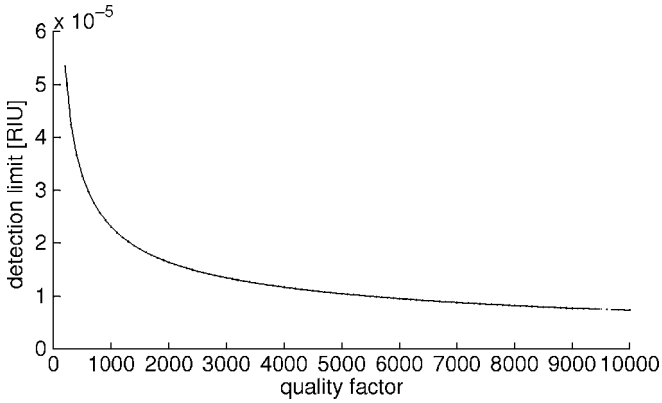

Fig. 6. Calculated influence of the quality factor of the resonator on the detection limit of the sensor for sensing refractive index changes of the complete top cladding.

noise. We then determined the detection limits corresponding to different widths of these theoretical resonance dips by using the fitting procedure explained in Section 4.1. Fig. 6 displays the impact of the quality factor on the detection limit, and shows us that an improvement of the quality factor of our resonator from its current value of 330 to a value of 1200 would already improve the detection limit with a factor 2. In order to achieve this increase of the quality factor, the resonator losses should be decreased.

In [15], a slot waveguide with SiO_2 top cladding made with the same fabrication process as our ring resonator is measured to have 12 dB/cm propagation loss. As the absorption of water at a wavelength of 1.55 μm is 47.5 dB/cm [16], and our simulations indicate that 20% of the waveguide mode power propagates through water, we can roughly estimate the propagation loss of our waveguide to be 12 dB/cm $+ 0.2 \cdot 47.5$ dB/cm $= 21.5$ dB/cm.

However, from the experimental transmission spectrum of our resonator at the pass port, we were able to extract 21.4 nm free spectral range, 0.082 transmission at resonance and a quality factor of 330, which allowed us to deduce a waveguide loss as high as 500 dB/cm, which is much higher than the predicted propagation loss for this waveguide. This indicates that the bend loss and mismatch loss (between bend and straight waveguide parts) are dominant over the propagation loss, and that an increase of the bend radius will thus have a large impact on the quality factor of our resonator and on its detection limit for biosensing.

Three-dimensional finite-difference time-domain simulations with the software package *Meep* [17] confirm that the slot waveguide bend loss is very high at a bend radius of 5 μm, and that increasing the bend radius from 5 to 12 μm reduces the bend loss from 160 to 20 dB/cm. Note that sidewall inclination, roughness, the presence of a biochemical layer, and absorption were not taken into account in these simulations due to the very high computational power demands, which can explain the difference between the experimentally and theoretically determined loss.

6. Conclusion

We numerically optimized SOI slot waveguides for label-free biosensing of proteins and presented a slot-waveguide-based ring resonator in SOI with a footprint of only 13 μm $\times$ 10 μm, fabricated with optical lithography. Experiments showed 298 nm/RIU sensitivity and a detection limit of $4.2 \cdot 10^{-5}$ RIU for refractive index changes of the complete top cladding. We proved for the first time that surface chemistry for selective label-free sensing of proteins can be applied inside a 100 nm-wide slot region and demonstrated that the application of a slot waveguide instead of a normal waveguide increases the sensitivity of an SOI ring resonator with a factor 3.5 for the detection of proteins. Finally, we proposed further enhancements of the sensor for an improvement of the detection limit.

Acknowledgment

The authors thank *ePIXfab* (www.epixfab.eu) for the fabrication of the device.

References

[1] X. Fan, I. M. White, S. I. Shopoua, H. Zhu, J. D. Suter, and Y. Sun, "Sensitive optical biosensors for unlabeled targets: A review," *Anal. Chim. Acta*, vol. 620, no. 1/2, pp. 8–26, Jul. 2008.
[2] P. Yager, T. Edwards, E. Fu, K. Helton, K. Nelson, M. R. Tam, and B. H. Weigl, "Microfluidic diagnostic technologies for global public health," *Nature*, vol. 442, no. 7101, pp. 412–418, Jul. 2006.
[3] K. De Vos, I. Bartolozzi, E. Schacht, P. Bienstman, and R. Baets, "Silicon-on-insulator microring resonator for sensitive and label-free biosensing," *Opt. Express*, vol. 15, no. 12, pp. 7610–7615, Jun. 2007.
[4] V. R. Almeida, Q. Xu, C. A. Barrios, and M. Lipson, "Guiding and confining light in void nanostructures," *Opt. Lett.*, vol. 29, no. 11, pp. 1209–1211, Jun. 2004.
[5] C. A. Barrios, K. B. Gylfason, B. Sánchez, A. Griol, H. Sohlström, M. Holgado, and R. Casquel, "Slot-waveguide biochemical sensor," *Opt. Lett.*, vol. 32, no. 21, pp. 3080–3082, Nov. 2007.
[6] C. A. Barrios, M. J. Banuls, V. Gonzalez-Pedro, K. B. Gylfason, B. Sanchez, A. Griol, A. Maquieira, H. Sohlstrom, M. Holgado, and R. Casquel, "Label-free optical biosensing with slot-waveguides," *Opt. Lett.*, vol. 33, no. 7, pp. 708–710, Apr. 2008.
[7] I. M. White and X. Fan, "On the performance quantification of resonant refractive index sensors," *Opt. Express*, vol. 16, no. 2, pp. 1020–1028, Jan. 2008.
[8] A. S. Sudbo, "Film mode matching: A versatile numerical method for vector mode field calculations in dielectric waveguides," *Pure Appl. Opt.*, vol. 2, no. 3, pp. 211–33, May 1993.
[9] J. Voros, "The density and refractive index of adsorbing protein layers," *Biophys. J.*, vol. 87, no. 1, pp. 553–561, Jul. 2004.
[10] S. Rauf, D. Zhou, C. Abell, D. Klenerman, and D. Kang, "Building three-dimensional nanostructures with active enzymes by surface templated layer-by-layer assembly," *Chem. Commun.*, no. 16, pp. 1721–1723, Apr. 2006.
[11] W. Bogaerts, D. Taillaert, B. Luyssaert, P. Dumon, J. V. Campenhout, P. Bienstman, D. V. Thourhout, R. Baets, V. Wiaux, and S. Beckx, "Basic structures for photonic integrated circuits in silicon-on-insulator," *Opt. Express*, vol. 12, no. 8, pp. 1583–1591, Apr. 2004.
[12] J. Blasco and C. Barrios, "Compact slot-waveguide/channel-waveguide mode-converter," in *Proc. CLEO/Eur.*, 2005, pp. 607–607.
[13] H. Su and X. G. Huang, "Fresnel-reflection-based fiber sensor for on-line measurement of solute concentration in solutions," *Sens. Actuators B, Chem.*, vol. 126, no. 2, pp. 579–582, Oct. 2007.
[14] K. De Vos, J. Girones, S. Popelka, E. Schacht, R. Baets, and P. Bienstman, "SOI optical microring resonator with poly(ethylene glycol) polymer brush for label-free biosensor applications," *Biosens. Bioelectron.*, vol. 24, no. 8, pp. 2528–33, Apr. 2009.
[15] C. Koos, P. Vorreau, T. Vallaitis, P. Dumon, W. Bogaerts, R. Baets, B. Esembeson, I. Biaggio, T. Michinobu, F. Diederich, W. Freude, and J. Leuthold, "All-optical high-speed signal processing with silicon-organic hybrid slot waveguides," *Nat. Photon.*, vol. 3, no. 4, pp. 216–219, Apr. 2009.
[16] K. Palmer and D. Williams, "Optical properties of water in the near infrared," *J. Opt. Soc. Amer.*, vol. 64, no. 8, pp. 1107–1110, Aug. 1974.
[17] A. Farjadpour, D. Roundy, A. Rodriguez, M. Ibanescu, P. Bermel, J. D. Joannopoulos, S. G. Johnson, and G. Burr, "Improving accuracy by subpixel smoothing in FDTD," *Opt. Lett.*, vol. 31, no. 20, pp. 2972–2974, Oct. 2006.